Drug Delivery

http://informahealthcare.com/drd
ISSN: 1071-7544 (print), 1521-0464 (electronic)

Drug Deliv, 2015; 22(1): 58–68
 DOI: 10.3109/10717544.2014.901436

informa
healthcare

RESEARCH ARTICLE

Linear-dendrimer type methoxy-poly (ethylene glycol)-b-poly (ε-caprolactone) copolymer micelles for the delivery of curcumin

Zhimei Song[1], Wenxia Zhu[1,2], Jiarong Song[3], Peng Wei[4], Fengying Yang[1], Na Liu[1], and Runliang Feng[1]

[1]Department of Pharmaceutical Engineering, School of biological science and technology, University of Jinan, Jinan, Shandong Province, PR China, [2]Shandong Academy of Medical Sciences, Jinan, Shandong Province, PR China, [3]Department of Pharmacy, The First Hospital of China Medical University, Heping District, Shenyang, Liaoning Province, PR China, and [4]National Laboratory of Biomacromolecules, Institute of Biophysics, Chinese Academy of Sciences, Chaoyang District, Beijing, PR China

Abstract

Purpose: To improve curcumin's pharmacokinetic, *in vitro* cytotoxicity and release property.
Methods: A novel linear-dendrimer methoxy-poly (ethylene glycol)-b-poly (ε-caprolactone) copolymer was synthesized through O-alkylation, basic hydrolysis and ring-opening polymerization reaction with methoxy-poly (ethylene glycol), epichlorohydrin and ε-caprolactone as raw materials. Its structure was characterized by ^{1}H-NMR and GPC. The copolymer's hemolysis and micellar encapsulation for curcumin by thin-film hydration were studied. Curcumin-loaded micelles were evaluated by use of *in vitro* release, FT-IR and X-ray diffraction. Curcumin-loaded micelles' *in vitro* cytotoxic activities against Hela and HT-29 cells were done, and its pharmacokinetic parameters were also carried out.
Results: Curcumin was encapsulated into the micelles with 92.54% of entrapment efficiency and 12.84% of drug loading in amorphous forms. The dissolubility of nanoparticulate curcumin was 1.70×10^5 times higher than that of curcumin in water. The obtained copolymer showed no hemolysis. *In vitro* drug release study indicated that, in all cases, the kinetics was adjusted well to the Makoid–Banakar model ($R^2_{abj} = 0.9984$). In addition, data were analyzed by the Korsmeyer–Peppas model, *n* values were 0.43, indicating that the drug release was accomplished by the combination diffusion and polymer chain relaxation. The cytotoxicity experiment indicated that the nanoparticulate curcumin kept up its potent anti-cancer activities. The pharmacokinetic results showed that the $MRT_{0-\infty}$, $t_{1/2z}$ and $AUC_{0-\infty}$ of Curcumin-loaded micelles were 1.64, 6.54 and 4.67 times higher than that of CUR control solution.
Conclusions: The copolymeric micelles loading curcumin might act as a delivery vehicle for CUR.

Keywords

ε-caprolactone, curcumin, delivery, linear-dendrimer, methoxy-poly(ethylene glycol), micelles

History

Received 11 February 2014
Revised 3 March 2014
Accepted 3 March 2014

Introduction

Curcumin (CUR) has several pharmacological activities such as antioxidant, -microbial and -tumor activities with low toxicity to human (Ono et al., 2004; Maheshwari et al., 2006). Previous studies about CUR have indicated its ability to induce apoptosis in cancer cells (Aggarwal et al., 2003). However, CUR's inferior solubility in water was its main obstacle to remain or improve bioavailability and clinical therapeutic effect (Letchford et al., 2008).

Extensive researches have focus on copolymeric micelles due to their stability and facility of surface modification (Avgoustakis et al., 2003; Sanyakamdhorn et al., 2014). Linear methoxy poly(ethylene glycol)-b-poly (ε-caprolactone) (MPEG-PCL) is a diblock copolymer that has distinct lipophilic and hydrophilous fragments, forming an internal lipophilic core and external hydrophilous shell due to their large solubility difference in aqueous medium. The CUR-loaded linear MPEG-PCL copolymeric micelles or micelles can obviously improve CUR's water-solubility, bioavailability, anti-tumor activity and forth (Mohanty et al., 2010; Gou et al., 2011; Shao et al., 2011; Gong et al., 2013; Yin et al., 2013).

It is noted that copolymers such as dendrimers (Medina & El-Sayed, 2009; Pan et al., 2009; Abderrezak et al., 2012), linear-*b*-dendritic block copolymers (Wurm & Frey, 2011), star block copolymers (Prabaharan et al., 2009a) and brush copolymers (Prabaharan et al., 2009b; Yan et al., 2009) have been studied as vehicles for drug loading and delivery. In comparison with linear polymers, these branched polymers have a greater effect on the physico-chemical characteristics of the polymer itself as well as drug delivery. In a former study, we have found that star-type MPEG-PCL obviously improve CUR's encapsulation and solubility in aqueous solution, and CUR release is slow and sustainable

Address for correspondence: Runliang Feng, Department of Pharmaceutical Engineering, School of Medicine and Life Sciences, University of Jinan, 336 Nanxinzhuang Xilu, Jinan 250022, Shandong Province, PR China. Tel: +86 531 89736825. Fax: +86 531 89736818. Email: runliangfeng@126.com

(Feng et al., 2013). It is believed that further modification of MPEG to provide a linear-dendrimer MPEG-PCL will also be helpful to CUR's encapsulation, release, increase of solubility in water, improvement of pharmacokinetic properties, as well as antitumor activity.

Herein, a linear-dendrimer MPEG-PCL copolymer was synthesized, characterized and used as a candidate polymer toward the development of an effective CUR drug delivery system in this study. CUR-loaded micelles (CUR micelles) were prepared from the copolymer's self-assembling aided by thin-film hydration. The physicochemical properties, *in vitro* release, hemolysis test, *in vitro* cytotoxicity and pharmacokinetics of CUR micelles were investigated in details as a potential drug delivery vehicle, respectively. The research results showed that both entrapment efficiency (EE) and DL of this linear-dendrimer MPEG-PCL were higher than that of linear MPEG-PCL for CUR reported by Mohanty et al. (2010). The CUR micelles obviously improved pharmacokinetic property of CUR while its cytotoxicity was kept. The CUR micelles would have a great prospective clinical application as a new injectable dosage form.

Materials and methods

Materials

Curcumin was bought from Fluka Chemical Company Inc. (Buchs, Switzerland). MPEG (Mn = 2000) was bought from Sigma Chemicals (St. Louis, MO) and dried twice by azeodistillation of toluene. ε-Caprolactone (ε-CL) was purchased from Huayuan Polymer Co. Ltd. (Qingdao, Shandong Province, China). Epichlorohydrin purchased from Tianjin Chemical Corp. (Tianjin, China) was used without further purification. Methylene dichloride and tetrahydrofuran (THF) were dried under sodium hydride and underwent distillation before use. All the other chemicals and solvents were of analytical grade or higher, obtained commercially.

Synthesis of tetra-hydroxyl MPEG

The tetra-hydroxyl MPEG was synthesized as previously (Lu et al., 2008). The procedure was described as follows: A three-neck flask equipped with a magnetic stirring bar was charged with MPEG (20 g, 10 mmol), sodium (2.3 g, 100 mmol) and 60 mL of THF. The reactants were aspirated at 60 °C for 10 h under nitrogen atmosphere. Then epichlorohydrin (5.55 g, 60 mmol) was injected and went on reaction at the same temperature for another 10 h. After being cooled to room temperature, the resultant mixture was filtered off and evaporated under vacuum to afford MPEG glycidyl ether.

The obtained MPEG glycidyl ether and 10% NaOH (140 mL, 389 mmol) were mixed and heated at 80 °C for 10 h. Then the mixture was evaporated to dry under vacuum, dissolved in 100 mL of acetonitrile and strained off. The organic phase filtrate was evaporated under vacuum to obtain di-hydroxyl MPEG as a white solid.

Then the di-hydroxyl MPEG was treated according to the procedure above to obtain tetra-hydroxyl MPEG with a yield of 89%.

Synthesis of linear-dendrimer MPEG-PCL diblock copolymer

The linear-dendrimer MPEG-PCL diblock copolymer was synthesized in accordance with published synthetic method of methosy-poly (ethylene glycol)-b-poly (δ-valerolactone) copolymer (Lee et al., 2005) and poly (ε-caprolactone)-b-poly (propylene glycol)-b-poly (ε-caprolactone) (Oh et al., 2009). To remove the last traces of water, the tetra-hydroxyl MPEG (5.0 g, 2.4 mmol) was azeotroped with toluene (20 mL) at 120 °C for 4 h in a three-neck flask. The toluene was removed by evaporation. To the residual dicloromethane (20 mL), 2 mol/L hydrochloride ethyl ether (4.8 mL) and different weight ratios of ε-CL were added in turn. After reaction at 25 °C for 24 h, resultant mixture was evaporated under vacuum and precipitated in 100 mL of ethyl ether to obtain the linear-dendrimer MPEG-PCL copolymer after filtration with a yield of 92%. It was marked LDMP.

The prepared tetra-hydroxyl MPEG and LDMP were characterized by FT-IR (KBr) (NEXUS 470, Nicolet, USA), ^{1}H-NMR (in $CDCl_3$) (AVANCE 300 MHz, Bruker, Germany) and GPC (in N, N-dimethylamino formide) (Waters 2690D-2410, Waters, MA).

Preparation of blank and CUR micelles

Micelles was formed by thin-film hydration (Wang et al., 2012a). The known weight of CUR and LDMP (weight ratio was 1:7) was co-dissolved in acetone. The solvent was removed under reduced pressure by rotary evaporation at room temperature to obtain a thin layer of uniform film on the wall of flask. The resulting yellowish thin film was hydrated with water under gentle agitation at 65 °C. The resulting solution was filtered through a 0.22-μm filter membrane and used for further analysis or lyophilization. Blank micelles were obtained in an analogous method.

Characterization of micelles

Critical micelle concentration of copolymer

Copolymer was accurately weighted and dissolved in deionized water at 25 °C and laid up for 24 h. By stepwise dilution, a series of LDMP solutions were provided as follow concentrations: 1×10^{-3}, 5×10^{-4}, 2×10^{-4}, 1×10^{-4}, 5×10^{-5}, 2×10^{-5}, 1×10^{-5}, 5×10^{-6}, 2×10^{-6}, 1×10^{-6}, 5×10^{-7}, 2×10^{-7} and 1×10^{-7} g/mL.

An equivalent volume of pyrene solution in acetone was added into a suite of volumetric flasks and organic solvent was purged by nitrogen flow. The LDMP solutions were added into the volumetric flasks to attain 2×10^{-6} mol/L of pyrene followed by balance at 60 °C and filtration through 0. 45 μm filter membrane before fluorescent measurements.

The fluorescence excitation spectrum was recorded on a fluorescent spectrophotometer (F-7000 FL, Hitachi Corp., Japan) from 300 to 360 nm with an emission wavelength of 390 nm under a bandwidth of 2.5 nm. Scanning speed was adjusted to 240 nm/min. Fluorescent spectra of pyrene assigned to a 0–0 vibration band showed great susceptibility to the environmental polarity. When micelles formed, pyrene would enter into micelles' inner core, resulting in a bathochromic shift of 0–0 vibration band from 336 to 338.5 nm.

The curve of strength rates ($I_{338.5}/I_{336}$) to copolymer concentration was used to obtain LDMP's critical micelle concentration (CMC) value from the point of intersection between the tangent of abrupt area and that of horizontal curve at low concentrations.

Morphology of blank and CUR micelles

Transmission electron microscope (TEM, JEM-1200EX, JEOL, Tokyo, Japan) was adopted for morphology observation. A copper wire mesh covered with carbon membrane (400 meshes) was submerged in micelles solution and then negatively stained with 2% phosphotungstic acid followed by absorption of redundant solution with absorbent paper and air drying prior to TEM experiment.

Particle size and zeta potential of blank and CUR micelles

Sizes of blank and CUR micelles were measured by Dynamic light scattering (DLS, Zetasizer 3000HS, Malvern Instruments Ltd., UK). The surface charge of the blank and CUR micelles suspension in deionized water was determined by Zeta potential. Results are donated as mean ± SD. All the experiments were repeated in triplicates.

Determination of EE and DL

The accurately weighted CUR micelles were added into ethanol in volumetric flask to disrupt the micellar core-shell structure and dissolve CUR releasing from the micelles, followed by stepwise dilution to afford a solution of CUR with UV absorbance at a range of 0.2–0.8. The quantitative analysis of CUR in the drug-loaded micelles was determined by use of ultraviolet spectrophotometry at 425 nm (T6 New Century, Purkinje General, Peking, China). The DL and EE were determined through applying equation as follow [Equations (1) and (2)] (Song et al., 2011):

$$\mathrm{EE} = \frac{\text{weight of drug in nanoparticles}}{\text{weight of the initial drug}} \times 100\% \qquad (1)$$

$$\mathrm{DL} = \frac{\text{weight of drug in nanoparticles}}{\text{weight of nanoparticles containing drug}} \times 100\% \qquad (2)$$

X-ray diffraction and FT-IR studies of CUR, blank and CUR micelles

X-ray diffraction (XRD) analysis was considered to identify the physical state of CUR in micelles. The XRD curves of CUR, lyophilized blank and CUR micelles were measured employing X-ray diffractometer (Bruker D8 Focus, Bruker, Germany) at a voltage of 40 kV and 25 mA with Cu K α radiation. The range of scanning angle was from 2.5° to 40° with a scanning speed of 2°/min.

FT-IR spectra were taken into observation to probe into the potential physico-chemical interactions between the CUR and the copolymer material. FT-IR spectrum of CUR, the lyophilized blank and CUR micelles were determined by KBr pellets method on a FT-IR spectrometer (NEXUS 470, Nicolet, USA) over the range from 4000 to 400 cm^{-1}, respectively.

Hemolysis test of copolymers

Hemolysis assay *in vitro* was employed to evaluate toxicity of LDMP copolymer (Cerda-Cristerna et al., 2011; Meng et al., 2011). Heparinized rat erythrocytes were separated from rat blood by centrifugation at 3000 r/min for 30 min in a centrifuge and eluted using physiological saline to achromatic color for supernatant solution. About 1 mL of the depurative erythrocytes was added into 39 mL of normal saline to a blood volume of 2.5%. About 1.6 mL of the resulting mixture was mixed with 4 mL of copolymer solution in physiological saline at 37 °C with shaking at 300 r/min for 30 min. The copolymer solution concentrations ranged from 156 to 2500 μg/mL. Physiological saline and aquadistillate were set as negative and positive control, respectively. After mix for 30 min, the mixtures were centrifuged for 20 min at 3000 r/min in order to separate intact red blood cells and disrupted membranes from the solution. The supernatant, containing the released hemoglobin (Hb), was collected. The absorbance of Hb in the supernatant at 500–650 nm was determined by UV-Vis spectrophotometer (T6 New Century, Purkinje General, Peking, China).

The hemolytic activities of LDMP micelles were evaluated based on absorbance at 576 nm. All determinations were done for three times (Dutta & Dey, 2011). The results were calculated based on Equation (3):

$$\text{Hemolysis } (\%) = \frac{\mathrm{Abs}_{\text{sample}} - \mathrm{Abs}_{\text{negative control}}}{\mathrm{Abs}_{\text{postive control}} - \mathrm{Abs}_{\text{negative control}}} \times 100\% \qquad (3)$$

In vitro release of CUR micelles

In vitro drug release behavior of CUR from CUR micelles was performed by dynamic dialysis method as explained in a literature (Sun et al., 2012). The study was conducted with the co-solvent mixture of physiological saline and absolute ethanol (60:40, V/V) as a release medium. As control, CUR was dissolved in propylene glycol. CUR micellar suspension or control solution (having 1 mg of CUR) was placed in dialysis bags (Viskas MD25-3.5, Union Carbide Corporation, Bound Brook, NJ), respectively. They were placed into beakers containing 100 mL of release mediums and shaken in a oscillation rate of 100 r/min at 37 °C. At each given time, 5 mL of the release mediums was taken out. About 5 mL of new release mediums was refilled to release medium. The amount of CUR released from the CUR micelles was determined by use of ultraviolet spectrophotometer at a wave-length of 425 nm (T6 New Century, Purkinje General, Peking, China). All measurements were performed in triplicates. The accumulative release percentage was calculated according to a reported calculation method (Li et al., 2013).

In vitro cytotoxicity of CUR micelles by MTT analysis

MTT method was used to evaluate the cytotoxicity of CUR micelles. In 96-well plates, Hela and HT-29 cells were seeded at a density of 5×10^4 cells/mL, then cultivated at 37 °C for 8 h in DMEM. The culture solution was replaced by 100 μL fresh medium containing different concentrations (0, 5, 10, 20 and 40 μM CUR/well) of either free CUR dissolved in DMSO or

equivalent concentration of CUR micelles (Ma et al., 2007). The incubation time was set as follow: 24 and 48 h. About 20 μL of MTT solution in PBS (5 mg/mL) was added to each well, and the cells were incubated for another 4 h at 37 °C in the darkness. The culture medium was removed and replaced with 100 μL DMSO to dissolve the blue formazan crystal; the percentage of cell viability was determined using a microplate reader (Model 680; Bio-Rad Laboratories, Hercules, CA) equipped with a 570-nm filter. All assays were conducted with four parallel samples.

Pharmacokinetics of CUR micelles

About 250 ± 20 g of male and female Wistar rats were bought from Shandong University (Jinan City, Shandong Province, China). All animal experiments complied with the requirements of the National Act on the use of experimental animals. Rats had no foodstuff and drank water freely for 12 h prior to experiments. They were randomly split into two groups (3/sex/group).

CUR control solution was prepared according to a reported article (Song et al., 2011). The rats were treated intravenously with control solution and CUR micelles through caudal vein at a dosage of 15 mg/kg, respectively. At every definite point of time, rat blood samples were gathered into heparinized tubes through dural sinus, and centrifuged at 5000 r/min for 5 min to separate plasma. The plasma samples were disposed according to a previous process (Ma et al., 2007).

Content of CUR in plasma was then determined with reported reversed-phase high-performance liquid chromatography (Shimadzu LC-10A, Japan) (Fang et al., 2009). A curve of plasma drug concentration to time was provided. Pharmacokinetic parameters were calculated by use of DAS 2.0 with non-compartmental model (Xu et al., 2010).

Result and discussion

Structure characterization of LDMP

Firstly, di-hydroxyl MPEG was synthesized by O-alkylation reaction of MPEG and epichlorohydrin followed by alkaline ring opening. Secondly, tetra-hydroxy MPEG was obtained through a repetitive operation above. At last, the LDMP was prepared by way of ring-opening copolymerization of tetra-hydroxyl MPEG and ε-CL under hydrochloride ether as a catalyst at room temperature (shown as Scheme 1).

The FT-IR spectrum of LDMP is shown in Figure 1. The peak at 1729 cm^{-1} indicated the existence of C=O stretching vibration of the ester carbonyl group being similar to that of ε-CL. The peaks at 1109 and 1244 cm^{-1} showed C–O–C stretching vibration of $–OCH_2CH_2$ elements of PEG and –COO– stretching vibration, respectively. The peaks at 2945 and 2870 cm^{-1} were belonged to the C–H stretching vibration of $–CH_2CH_2$, respectively, which were similar to ε-CL.

The ^{1}H-NMR spectrum of tetra-hydroxyl MPEG is shown as Figure 2(A). The sharp peak at 3.38 (a) was attributed to methyl protons of tetra-hydroxyl MPEG. The strong peak at 3.64 (b) indicated methylene protons of tetra-hydroxyl MPEG. The single broad peak at 3.99 ppm (c) was hydro proton resonances of methenyl. Peaks of methylene protons adjacent to these methenyl were 3.81, 3.55 and 3.46 ppm, respectively. In addition, the terminal hydroxy peaks appeared at 2.01 ppm.

According to the ^{1}H-NMR spectrum of LDMP shown in Figure 2(B), the methylene protons (b) of the MPEG segment was found at 3.65 ppm. The peak at 3.38 ppm was identified as the $–OCH_3$ proton (a) of MPEG end unit. The hydroxyl peak at 2.01 disappeared, showing that the tetra-hydroxy MPEG reacted with ε-CL. The four new peaks present at 1.39, 1.63, 2.32 and 4.06 ppm after ring-opening polymerization reaction were assigned to the methylene protons of $OCOCH_2CH_2$–**CH_2**–CH_2CH_2, $OCOCH_2$–**CH_2**–CH_2–**CH_2**–CH_2, OCO–**CH_2**–$(CH_2)_4$ and $OCOCH_2CH_2CH_2CH_2$–**CH_2** in PCL units, respectively, being very similar to the reported spectrum (Jia et al., 2008; Zhou et al., 2003).

Figure 3 is the typical GPC curve of LDMP-2 copolymer. The weight average molecular weight was 13 461 with 2.05 of polydispersion index. It could be found that only a single peak existed at 22.62 min, suggesting the monodispersity of macromolecular weight and no other side-reactions during polymerization (Sahu et al., 2008).

Characterization of micelles

In order to select an ideal dosage form with better encapsulation, we prepared CUR micelles on the basis of LDMP and researched the influence of PCL chain length on DL and EE. From results listed in Table 1, the DL and EE rised with the raise of PCL length (changing from LDMP-1 to LEMP-3). The EE for LDMP-1 was 87.82 ± 3.03%, however, obvious precipitate appeared when stored overnight. The maximum EE reached to ~92.5% for LDMP-2, in which the length of PCL chain was higher than that in LDMP-1. The DL and EE did not obviously change with the further rise of PCL chain length (changing from LDMP-2 to LDMP-3). MPEG is a

Scheme 1. Synthesis of LDMP.

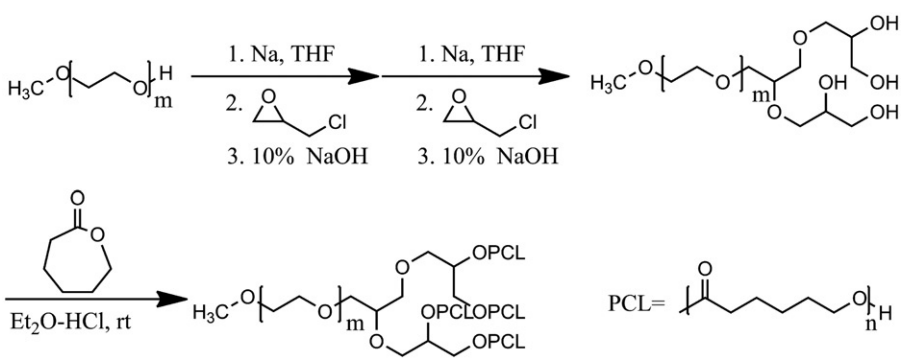

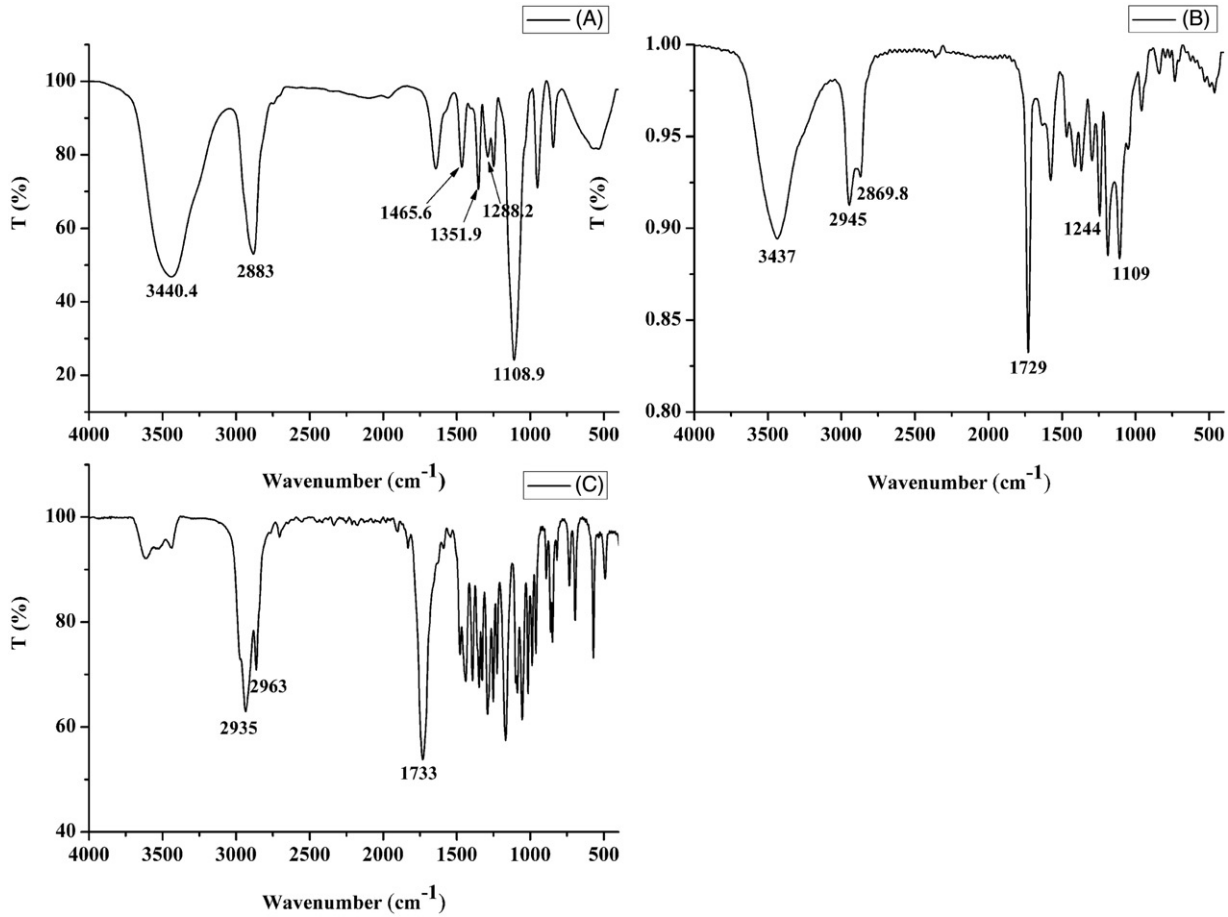

Figure 1. FT-IR spectrum of MPEG (A), LDMP (B) and ε-CL (C).

water soluble hydrophilic polymer forming outer shell, PCL is a hydrophobic chain forming inner core in water (Hu et al., 2003). The formed LDMP also contained MPEG and PCL, showing that it was also amphiphilic copolymer. It could also form a core-shell structure by use of thin-film hydration. Amphiphilic LDMP copolymer could also self-assembly form micelles with core-shell structure under water condition. The lipophilic CUR should be encapsulated into inner core by way of intermolecular hydrophobic interactions of CUR with PCL, and the drug was dissolved in water under hydration of PEG outer shell in aqueous medium (Letchford et al., 2008). Consequently, the stronger intermolecular interactions between the longer PCL block chain and lipophilic CUR might result in the higher DL and EE of CUR in LDMP. However, further increase of the PCL chain length might reduce water-solubility of the copolymer, resulting in the lower encapsulation of CUR. The LDMP-2 was selected for the further research according to its higher DL, EE and smaller mean particle diameter.

The LDMP-2's CMC was 2.18×10^{-6} g/mL, indicating that LDMP copolymer could form micelles at a lower copolymer concentration.

In this study, UV-Vis spectrophotometer was selected for quantitative analysis of CUR (without results shown). The result of UV-Vis analysis indicated that the DL and EE of CUR micelles prepared from LDMP-2 was 12.84% and 92.54% for LDMP-2, respectively. The total volume of CUR micelles solution was 4.8 mL. The water solubility of CUR in CUR micelles was increased to 1.87 mg/mL, which was 1.70×10^5 times higher than that of CUR in aqueous medium (Yallapu et al., 2010). The zeta potential of the CUR micelles was -9.26 ± 1.30 mV. The mean particle size of this CUR micelles obtained from DLS was 108.3 ± 13.6 nm. The TEM picture of CUR micelles showed that the micelles had a discontinuous spherical outline (Figure 4).

To confirm the presence of drug in CUR micelles, FT-IR spectrum analysis was performed. Figure 5 lists the FT-IR spectrums of CUR, lyophilized CUR-free and -loaded micellar particles. Peak of free CUR at 3508 cm^{-1} was assigned to the stretching vibration of phenolic hydroxyl group (Yen et al., 2010; Xie et al., 2011). In comparison with the blank micellar particles' C=O stretching vibration bond at 1729 cm^{-1}, the C=O absorption band blue shift of CUR micellar particles took place (Figure 5). At the same time, the phenolic hydroxyl group absorption band of CUR disappeared. These results indicated that intermolecular hydrogen bonds were formed between the C=O bond of LDMP and the O–H bond of CUR (Yallapu et al., 2010).

In case of CUR, sharp absorption bands at 1629, 1595, 1508, 1428 and 1277 cm^{-1} were indicated to be olefinic C=C, aromatic C=C stretching vibrations, C–O/C–C vibrations, olefinic C–H bending vibration and aromatic C–O stretching vibration, respectively (Mohanty & Sahoo, 2010). The signature peaks at 1627, 1587, 1515 and 1423 cm^{-1} due to C=C double bonds, aromatic C=C double bonds, C–O/

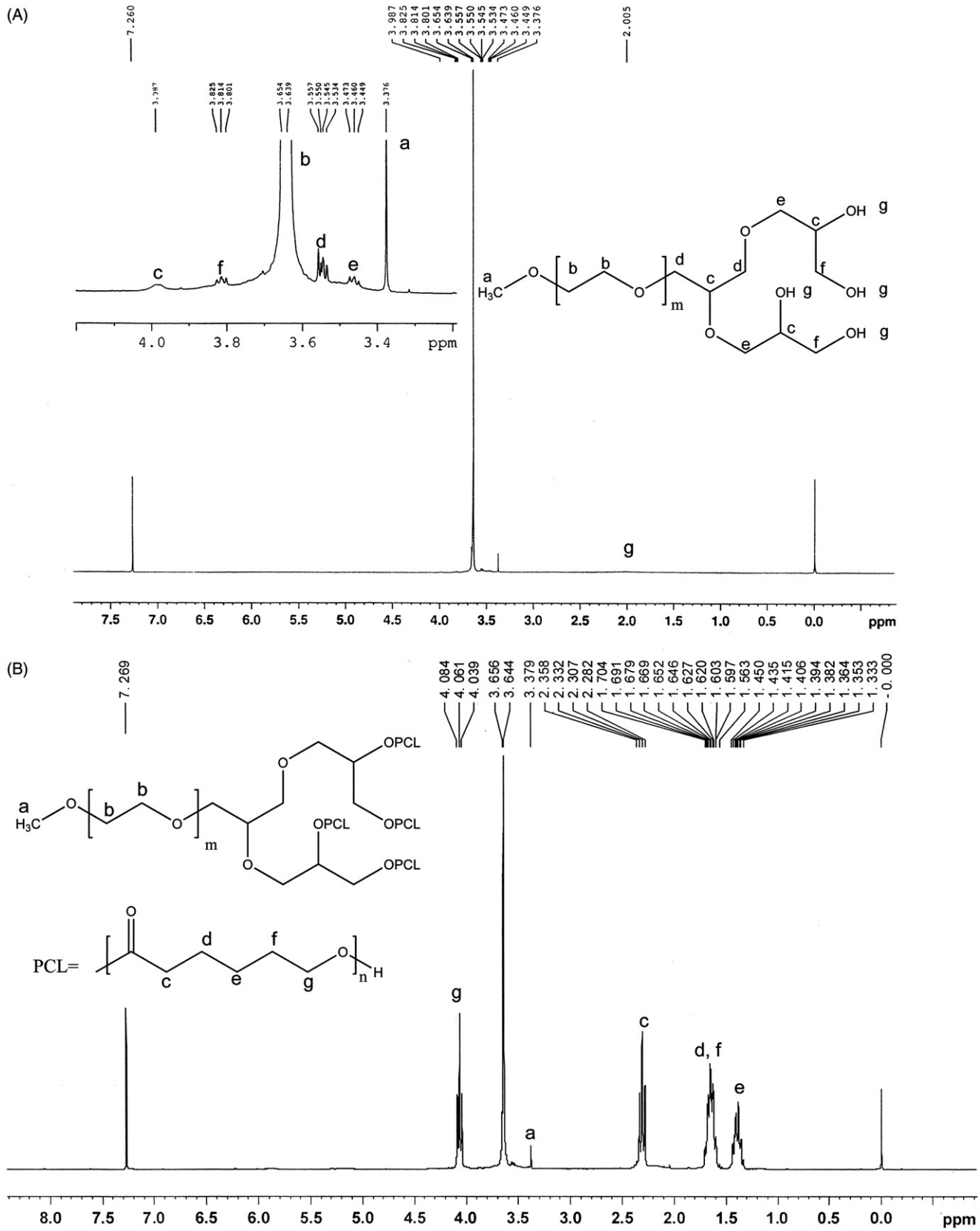

Figure 2. ^{1}H-NMR spectrum of tetra-hydroxy MPEG (A) and LDMP (B).

C–C vibrations and olefinic C–H bending vibration were also found in the FT-IR spectrum of CUR micellar particles, respectively. These peaks were similar to the absorption bands of CUR described above. However, they were absent in CUR-free micellar particles (Figure 5). These research results suggested that CUR could exist in dispersed state in case of CUR micelles formed from LDMP (Zhang et al., 2010b).

X-ray diffraction measurement was also used to confirm the physical state of CUR in micelles, because the exitential state of drug in the copolymeric materials of micelles was important to the drug release characteristics (Donsi et al., 2010; Yen et al., 2010). XRD spectra of CUR, CUR-free micelles and CUR micelles are shown in Figure 6. In Figure 6, the characteristic XRD peaks of CUR appeared at a series of diffraction angles 2θ at 8.84°, 12.14°, 14.46°, 17.26°, 18.12°, 21.14°, 23.36°, 24.50°, 25.54°, 27.34°, 28.14° and 28.96°, which indicated that pure CUR was in a highly crystalline form (Zhang et al., 2010b). However, no characteristic CUR peaks were detected in case of CUR micelles (Figure 6). This disappearance of characteristic peaks of CUR in CUR micelles dosage clearly implied that there were no CUR crystals in the CUR micelles. So, it could be inferred that CUR in CUR micelles dosage was in non-crystalline, unordered crystallographic phase or in solid solution state (Zhang et al., 2010b) which helped easy diffusion of CUR through the copolymeric material, resulting in a controlled release of CUR.

Hydrophobic species are known to interact with lipid cell membranes, resulting in its attachment to cell and finally endosomal uptake of hydrophobic substances. However, it can also lead to damage of cell membranes (so-called cytotoxic side effects) when these interactions are too intensive. To evaluate the biocompatibility of the copolymers, the change of hemolytic activity as a function of the concentration of the copolymers was performed against rat red blood cells. The hemoglobin absorption spectrum after mixture and hatch with the polymers is shown in Figure 7(A). It was seen that there were two UV-Vis absorption peaks of red blood cells at ~541 and 576 nm. The haemolytic activities of LDMP-2 micelles were evaluated based on absorbance at 576 nm. Results from the Figure 7(B) showed that no apparent hemolytic activity was observed in 156~2500 μg/mL, in which the hemolysis (%) was among 0–4.69% (<5%) at 576 nm (Letchford et al., 2008).

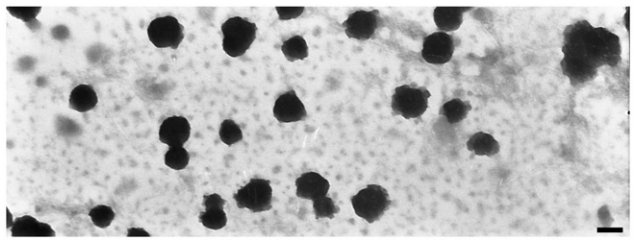

Figure 4. TEM of CUR micelles (38 000×, the scale bar is 100 nm).

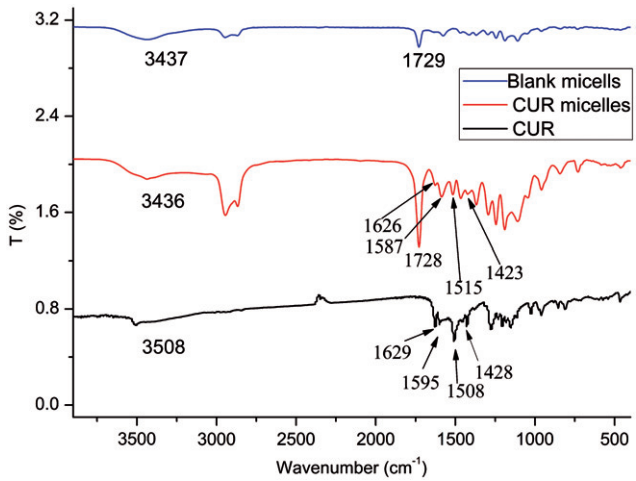

Figure 5. FT-IR spectrum of CUR, blank micelles and CUR micelles.

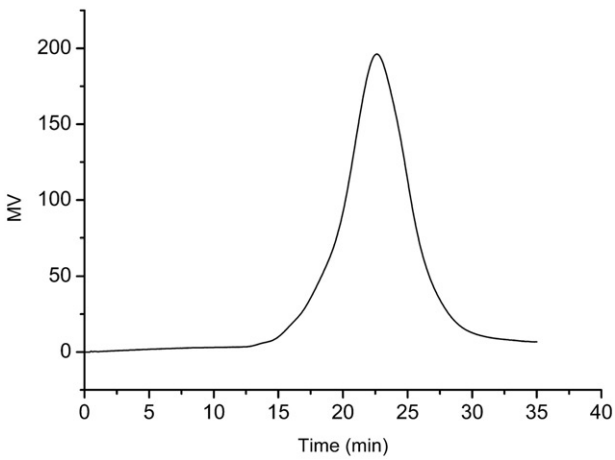

Figure 3. GPC of LDMP-2.

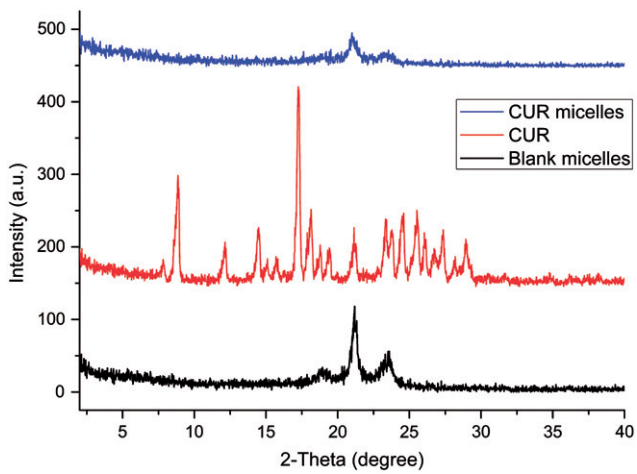

Figure 6. XRD of CUR, blank micelles and CUR micelles.

Table 1. Characteristics of micelles.

Micelles	Feed ratio	Mw theo	Mw GPC	DPI	EE (%)	DL (%)	Mean particle (nm)
LDMP-1	1:0.5	3000	10 868	1.733	87.82 ± 3.03	10.28 ± 0.42	Precipitation
LDMP-2	1:2	6000	13 461	2.050	92.54 ± 0.54	12.84 ± 0.29	108.3 ± 13.6
LDMP-3	1:3	8000	23 942	2.016	92.53 ± 1.10	12.71 ± 0.28	146.7 ± 10.1

Mw theo, theoretical molecular weight obtained from weight ratio of MPEG and ε-CL charge.

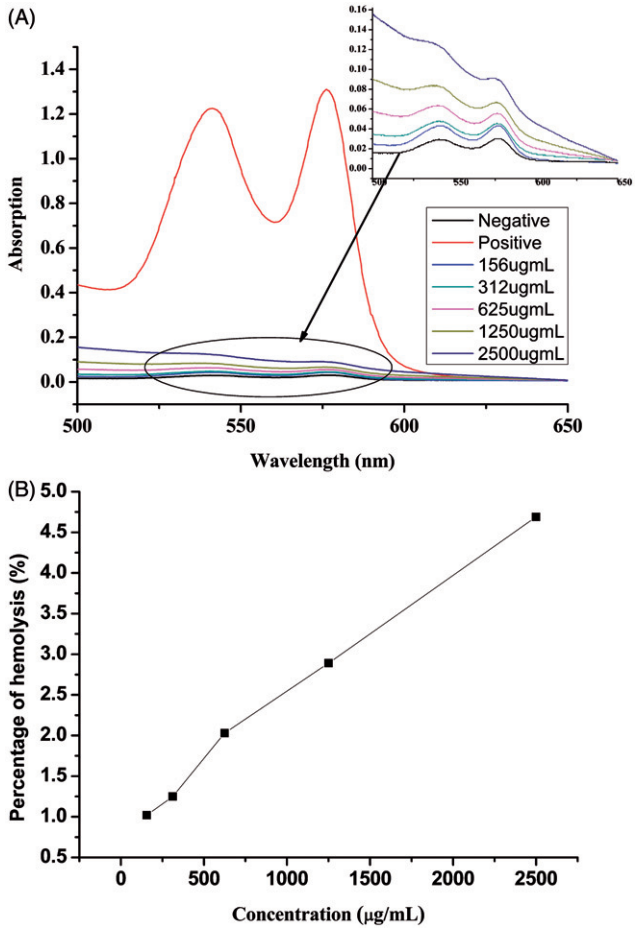

Figure 7. (A) Hemolysis test UV spectrum of different concentration of LMP, normal saline (negative control), and distilled water (positive control) and (B) percentage of hemolysis of different concentration of LDMP-2.

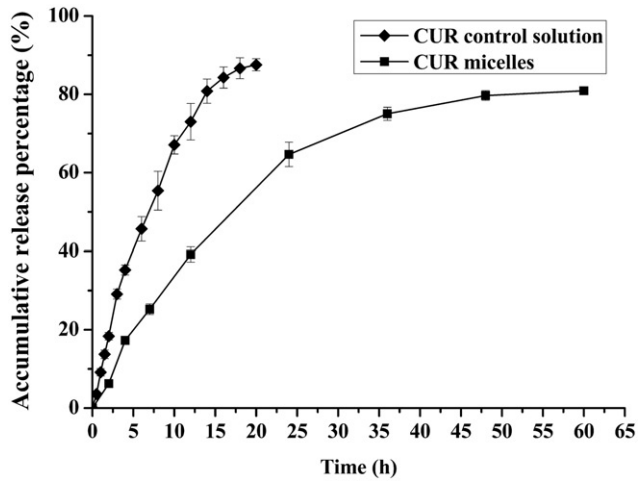

Figure 8. *In vitro* CUR-release profiles from either control solution or micelles in 40% ethanol saline solution at 37 °C [data are presented as mean ± SD ($n = 3$)].

In vitro release of CUR micelles

It is necessary for dosage form design that a drug can be easily discharged from drug-loaded copolymeric micelles because a limited release will hinder the drug's availability and then lead to reduction of its curative effect. Therefore, dynamic membrane dialysis method was adopted to investigate the release behavior of CUR from LDMP micelles. On account of the lower dissolvability of CUR in aqueous medium (Zhang et al., 2010a), a co-solvent of ethanol-physical saline solution (40:60, V/V) was used as the dialysis medium to provide a sink condition. The *in vitro* release behaviors of CUR control solution and CUR micelles in 40% (V/V) of ethanol saline solution are presented in Figure 8. The release results demonstrated that the release of CUR from control solution through dialysis membrane was much faster, 87.54% of CUR was released in 20 h. In contrast, only ~64.66% of CUR was released from CUR micelles within 24 h. Subsequently, the release rate became smaller and smaller, showing a sustained-release property and the accumulative release percentage at 60 h was ~80.91%.

To investigate and comprehend the phenomena referring to the release process, we fitted the release curve of CUR micelles with employment of different release models according to the reported DDsolver Add-in Program (Table 2) (Sharma et al., 2011). For LDMP micelles, the expressions that allowed a good fitting for the drug-release were Makoid–Banakar, Peppas–Sahlin, Quadratic, Weibull and Logistic models ($R^2_{abjusted} > 0.99$) (Table 2). The best fitted release kinetics model for LDMP micelles was the Makoid–Banakar model with $R^2_{abjusted} = 0.9984$ (Table 2), because its Akaike information criterion (AIC) value was the lowest and model selection criteria (MSC) value was the largest among these release models. These finding suggested that the release of CUR from micelles was mainly controlled by diffusion and polymer material erosion (Sanna et al., 2011).

To further understand the mechanism of the CUR release, the release behavior was also fitted by the Korsmeyer–Peppas model (Mohanty et al., 2010). Shown as Table 2, the CUR micelles under this study showed an n value of 0.535. The result implied that the CUR release was achieved by the cooperation of drug diffusion with copolymer chain relaxation (Prasanna et al., 2011; Seremeta et al., 2013). For the CUR micelles, early stage release should mainly rely on CUR's diffusion through polymeric framework, and diffusion taking place near to micelles' surface resulted in sudden release). Later stage release should be controlled by both diffusion of CUR and polymer chain relaxation resulted from degradation of the polymeric framework (Puga et al., 2012).

Cytotoxicity studies

Cytotoxicity of free CUR and CUR micelles was evaluated by MTT method in the HT-29 and Hela cell lines *in vitro*. As shown in Figure 9, CUR micelles showed no cytotoxicity compared with free CUR during 24 h. After incubation for 48 h, the CUR micelles obviously decreased the viability of both two cell lines with the increase of drug concentration. But it was shown that the anticancer activity effect of CUR micelles was not significantly different from free CUR. The possible reason might be that CUR was encapsulated into the copolymer to form micelles which raised cell ingestion of CUR micelles, but the slower release of drug from micelles would maintain CUR in a lower concentration than that of

Table 2. Mathematical equations for the models used to describe release characteristics of CUR from micelles.

Model	Equation	Parameter	$R^2_{adjusted}$	AIC	MSC
Zero order model	$Q_R = k_0 t$	$k_0 = 1.710$	0.7808	69.7396	1.0475
One order model	$Q_R = 100(1 - e^{-k_1 t})$	$k_1 = 0.038$	0.9834	46.5249	3.6269
Higuchi model	$Q_R = k_H t^{1/2}$	$k_H = 11.357$	0.9612	54.1590	2.7787
Korsmeyer–Peppas model	$Q_R = k_{KP} t^n$	$k_{KP} = 0.535$ $n = 0.535$	0.9578	55.7022	2.6072
Hixson–Crowell model	$Q_R = 100[1-(1-k_{HC}t)^3]$	$k_{HC} = 0.01$	0.9541	55.6635	2.6115
Hopfenberg model	$Q_R = 100[1-(1-k_{HB}t)^n]$	$K_{HB} = 0$ $n = 6321.872$	0.9810	48.5297	3.4042
Baker–Lonsdale model	$1.5\left[1 - \left(1 - \frac{Q_R}{100}\right)^{2/3}\right] - \frac{Q_R}{100} = k_{BL} t$	$k_{BL} = 0.003$	0.9470	56.9698	2.4664
Makoid–Banakar model	$Q_R = k_{MB} t^n e^{-kt}$	$k_{MB} = 4.215$ $n = 0.994$ $k = 0.019$	0.9984	27.0167	5.7945
Peppas–Sahlin model	$Q_R = k_1 t^m + k_2 t^{2m}$	$k_1 = 5.066$ $k_2 = -0.079$ $m = 0.883$	0.9969	32.9048	5.1403
Quadratic model	$Q_R = 100(k_1 t^2 + k_2 t)$	$k_1 = 0$ $k_2 = 0.035$	0.9911	41.6970	4.1634
Weibull model	$Q_R = 100(1 - e^{-\frac{(t-T_i)^\beta}{\alpha}})$	$\alpha = 11.315$ $\beta = 0.756$ $T_i = 1.414$	0.9918	41.5820	4.1761
Logistic model	$Q_R = 100 \times \frac{e^{(\alpha+\beta \log t)}}{1+e^{(\alpha+\beta \log t)}}$	$\alpha = -3.449$ $\beta = 2.866$	0.9963	33.7019	5.0517

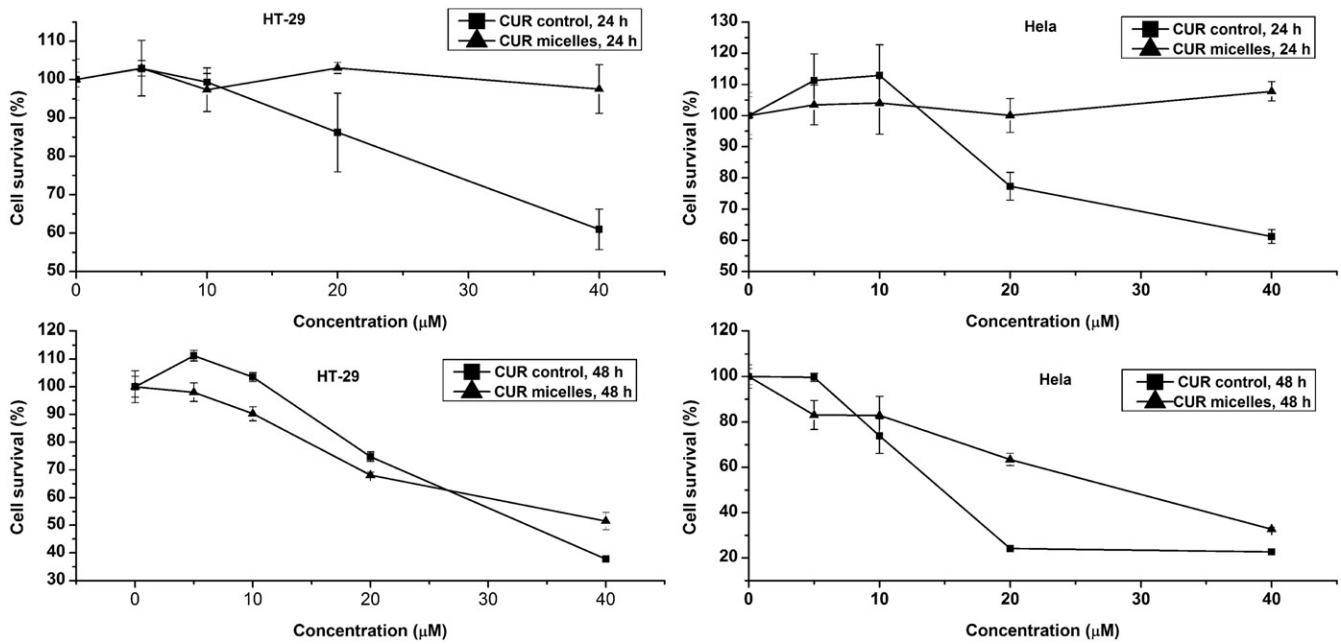

Figure 9. Anticancer activity of free CUR and CUR micelles on HT-29 and Hela cells *in vitro* after cultivation for 24 and 48 h [data are presented as mean ± SD ($n = 4$)].

free CUR in these cells (Costa & Sousa Lobo, 2001). The release of CUR from micelles was very slow in the first 24 h, resulting in no cytotoxicity. During subsequent 24 h, the release amount of CUR was obviously increased, leading to its accumulation and anticancer activity enhancement. The results demonstrated that the encapsulation of CUR in polymeric micelles had anticancer effect on HT-29 and Hela cells.

Pharmacokinetics of CUR micelles

The LDMP-2 was selected to investigate pharmacokinetic effects of CUR micelles on the basis of its higher EE and DL. The drug–time curves of CUR control solution and CUR micelles are presented in Figure 10. The time of duration for CUR control solution was ~1.5 h, but CUR micelles could obviously prolong cycling time of CUR for 6 h.

The pharmacokinetic parameters were analyzed according to ''DAS 2.0 practical pharmacokinetics program'' by non-compartmental model. The pharmacokinetic parameters, such as $AUC_{0-\infty}$, $MRT_{0-\infty}$, CL_z, V_z and $t_{1/2Z}$, are listed in Table 3.

From results listed in Table 3, the pharmacokinetic parameters of CUR micelles in rats were significantly different from these of the CUR control solution. $AUC_{0-\infty}$ for CUR micelles (4464.601 μg/L h) was ~4.62-fold higher

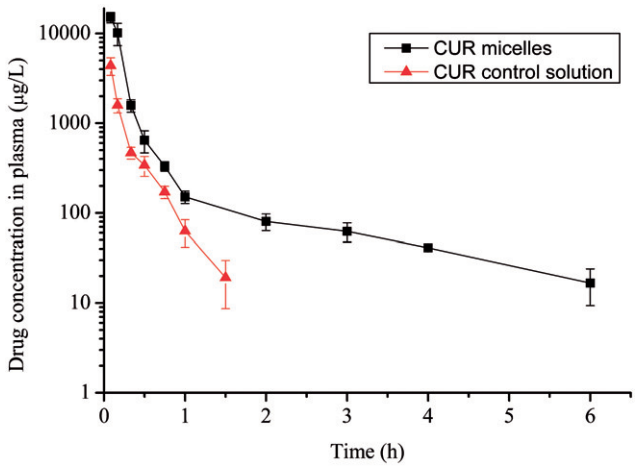

Figure 10. Drug–time curves after i.v. injection of CUR control solution and CUR micelles [data are presented as mean ± SD ($n = 6$)].

Table 3. Pharmacokinetic parameters of CUR control solution and CUR micelles ($n = 6$).

Parameters	CUR control solution	CUR micelles
$AUC_{0-\infty}$ (μg/L h)	967.221	4464.601
$MRT_{0-\infty}$ (h)	0.199	0.327
$t_{1/2Z}$ (h)	0.198	1.294
CL_Z (L/h/kg)	15.508	3.36
V_Z (L/kg)	4.432	6.271

than that of CUR solution. $MRT_{0-\infty}$, (0.327 h) was longer than that of CUR control solution. CUR micelles could also lengthen the half-time ($t_{1/2z} = 1.294$) of CUR in plasma which was 6.54-fold longer than that of CUR control solution. The CUR micelles also reduced CL_z in comparison with CUR control solution. The longer $MRT_{0-\infty}$ and lower CL_z manifested that CUR micelles could extend cycling time of CUR *in vivo*, and then led to longer acting time. The V_Z of CUR loaded within CUR micelles (6.271 L/kg) was evidently larger than that within CUR control solution (4.432 L/kg). This result made clear that CUR micelles could extend the retention time and delay clearance of CUR. The more micelles can circulate in blood for a longer period, the greater their accumulation in tumor may occur.

The possible reason was that micelles coated with hydrophilic polymer had a reduced opsonization and a longer period in circulation (Liu et al., 2012; Wang et al., 2012b). High mobility of linear poly (ethylene oxide) chains in LDMP-2 might present to repel approaching proteins from the particle surface because the protein does not have sufficient contact time with the mobile chains (Ghosh & Ryan, 2013), which delayed the residence time of CUR in blood. In our study, CUR plasma concentration could be still detected at 6-h post-injection of CUR-NS, but only up to 1.5 h for CUR control solution. Thus, CUR-NS could maintain a longer retention time in blood compared to CUR control solution.

Conclusion

The novel linear-demdrimer LDMP copolymer was synthesized by O-alkylation, basic hydrolysis and ring-opening polymerization reaction with MPEG, epichlorohydrin and ε-CL as raw materials. The obtained copolymer showed no apparent hemolytic activity. The formed CUR micelles could obviously increase CUR's solubility in water and afford an appropriate sustained-release property while the cytotoxicity *in vitro* remained comparable to that of free CUR. The entrapment of CUR in the linear-dendrimer copolymeric micelles markedly improved the pharmacokinetic properties. Hence, the micelles formulation is an outstanding solubilizer and hopefully a potential vehicle for the CUR delivery for cancer treatment in the future.

Declaration of interest

This work is supported by the Excellent Middle and Young Scientist Award Fund of Shandong Province, China (BS2011CL006), Scientific Research Fund of University of Jinan (XKY1208) and Research Fund for the Doctoral Program of University of Jinan (XBS1203). The authors report no conflicts of interest in this work.

References

Abderrezak A, Bourassa P, Mandeville JS, et al. (2012). Dendrimers bind antioxidant polyphenols and cisplatin drug. PLoS One 7:e33102.
Aggarwal BB, Kumar A, Bharti AC. (2003). Anticancer potential of curcumin: preclinical and clinical studies. Anticancer Res 23:363–98.
Avgoustakis K, Beletsi A, Panagi Z, et al. (2003). Effect of copolymer composition on the physicochemical characteristics, in vitro stability, and biodistribution of PLGA-mPEG nanoparticles. Int J Pharm 259: 115–27.
Cerda-Cristerna BI, Flores H, Pozos-Guillén A, et al. (2011). Hemocompatibility assessment of poly(2-dimethylamino ethylmethacrylate) (PDMAEMA)-based polymers. J Control Rel 153:269–77.
Costa P, Sousa Lobo JM. (2001). Modeling and comparison of dissolution profiles. Eur J Pharm Sci 13:123–33.
Donsi F, Wang Y, Li J, Huang Q. (2010). Preparation of curcumin submicrometer dispersions by high-pressure homogenization. J Agric Food Chem 58:2848–53.
Dutta P, Dey J. (2011). Drug solubilization by amino acid based polymeric nanoparticles: characterization and biocompatibility studies. Int J Pharm 421:353–63.
Fang L-N, Chen X-H, Song Z, et al. (2009). Development of a high performance liquid chromatography method for quantification of PAC-1 in rat plasma. J Pharm Biomed Anal 49:447–50.
Feng R, Zhu W, Song Z, et al. (2013). Novel star-type methoxy-poly(ethylene glycol) (PEG)-poly(ε-caprolactone) (PCL) copolymeric nanoparticles for controlled release of curcumin. J Nanoparticle Res 15:1–12.
Ghosh M, Ryan RO. (2013). ApoE enhances nanodisk-mediated curcumin delivery to glioblastoma multiforme cells. Nanomedicine.
Gong C, Deng S, Wu Q, et al. (2013). Improving antiangiogenesis and anti-tumor activity of curcumin by biodegradable polymeric micelles. Biomaterials 34:1413–32.
Gou M, Men K, Shi H, et al. (2011). Curcumin-loaded biodegradable polymeric micelles for colon cancer therapy in vitro and in vivo. Nanoscale 3:1558–67.
Hu Y, Jiang X, Ding Y, et al. (2003). Preparation and drug release behaviors of nimodipine-loaded poly(caprolactone)-poly(ethylene oxide)-polylactide amphiphilic copolymer nanoparticles. Biomaterials 24:2395–404.
Jia W, Gu Y, Gou M, et al. (2008). Preparation of biodegradable polycaprolactone/poly (ethylene glycol)/polycaprolactone (PCEC) nanoparticles. Drug Deliv 15:409–16.
Lee H, Zeng F, Dunne M, Allen C. (2005). Methoxy poly(ethylene glycol)-block-poly(delta-valerolactone) copolymer micelles for formulation of hydrophobic drugs. Biomacromolecules 6:3119–28.
Letchford K, Liggins R, Burt H. (2008). Solubilization of hydrophobic drugs by methoxy poly(ethylene glycol)-block-polycaprolactone diblock copolymer micelles: theoretical and experimental data and correlations. J Pharm Sci 97:1179–90.

Li Y, Xu X, Shen Y, et al. (2013). Preparation and evaluation of copolymeric micelles with high paclitaxel contents and sustained drug release. Colloids Surf Physicochem Eng Aspects 429:12–18.

Liu L, Sun L, Wu Q, et al. (2012). Curcumin loaded polymeric micelles inhibit breast tumor growth and spontaneous pulmonary metastasis. Int J Pharm 443:175–82.

Lu DD, Yuan JC, Li H, Lei Z-Q. (2008). Synthesis and characterization of a series of biodegradable and biocompatible PEG-supported poly(lactic-ran-glycolic acid) amphiphilic barbell-like copolymers. J Polym Sci A Polym Chem 46:3802–12.

Ma Z, Shayeganpour A, Brocks DR, et al. (2007). High-performance liquid chromatography analysis of curcumin in rat plasma: application to pharmacokinetics of polymeric micellar formulation of curcumin. Biomed Chromatogr 21:546–52.

Maheshwari RK, Singh AK, Gaddipati J, Srimal RC. (2006). Multiple biological activities of curcumin: a short review. Life Sci 78:2081–7.

Medina SH, El-Sayed MEH. (2009). Dendrimers as carriers for delivery of chemotherapeutic agents. Chem Rev 109:3141–57.

Meng H, Xue M, Xia T, et al. (2011). Use of size and a copolymer design feature to improve the biodistribution and the enhanced permeability and retention effect of doxorubicin-loaded mesoporous silica nanoparticles in a murine xenograft tumor model. ACS Nano 5: 4131–44.

Mohanty C, Acharya S, Mohanty AK, et al. (2010). Curcumin-encapsulated MePEG/PCL diblock copolymeric micelles: a novel controlled delivery vehicle for cancer therapy. Nanomedicine 5: 433–49.

Mohanty C, Sahoo SK. (2010). The in vitro stability and in vivo pharmacokinetics of curcumin prepared as an aqueous nanoparticulate formulation. Biomaterials 31:6597–611.

Oh JM, Lee SH, Son JS, et al. (2009). Ring-opening polymerization of ε-caprolactone by poly(propyleneglycol) in the presence of a monomer activator. Polymer 50:6019–23.

Ono K, Hasegawa K, Naiki H, Yamada M. (2004). Curcumin has potent anti-amyloidogenic effects for Alzheimer's beta-amyloid fibrils in vitro. J Neurosci Res 75:742–50.

Pan B, Cui D, Xu P, et al. (2009). Synthesis and characterization of polyamidoamine dendrimer-coated multi-walled carbon nanotubes and their application in gene delivery systems. Nanotechnology 20: 125101.

Prabaharan M, Grailer JJ, Pilla S, et al. (2009a). Amphiphilic multi-arm-block copolymer conjugated with doxorubicin via pH-sensitive hydrazone bond for tumor-targeted drug delivery. Biomaterials 30: 5757–66.

Prabaharan M, Grailer JJ, Pilla S, et al. (2009b). Folate-conjugated amphiphilic hyperbranched block copolymers based on Boltorn® H40, poly(l-lactide) and poly(ethylene glycol) for tumor-targeted drug delivery. Biomaterials 30:3009–19.

Prasanna R, Chinnakonda Chandramoorthy H, Ramaiyapillai P, Sakthisekaran D. (2011). In vitro evaluation of anticancer effect of Cassia auriculata leaf extract and curcumin through induction of apoptosis in human breast and larynx cancer cell lines. Biomed Prev Nutr 1:153–60.

Puga AM, Rey-Rico A, Magarinos B, et al. (2012). Hot melt poly-epsilon-caprolactone/poloxamine implantable matrices for sustained delivery of ciprofloxacin. Acta Biomater 8:1507–18.

Sahu A, Bora U, Kasoju N, Goswami P. (2008). Synthesis of novel biodegradable and self-assembling methoxy poly(ethylene glycol)-palmitate nanocarrier for curcumin delivery to cancer cells. Acta Biomater 4:1752–61.

Sanna V, Roggio AM, Posadino AM, et al. (2011). Novel docetaxel-loaded nanoparticles based on poly(lactide-co-caprolactone) and poly(lactide-co-glycolide-co-caprolactone) for prostate cancer treatment: formulation, characterization, and cytotoxicity studies. Nanoscale Res Lett 6:260–9.

Sanyakamdhorn S, Chanphai P, Tajmir-Riahi HA. (2014). Encapsulation of biogenic and synthetic polyamines by nanoparticles PEG and mPEG-anthracene. J Photochem Photobiol B 130:30–9.

Seremeta KP, Chiappetta DA, Sosnik A. (2013). Poly(epsilon-caprolactone), Eudragit(R) RS 100 and poly(epsilon-caprolactone)/Eudragit(R) RS 100 blend submicron particles for the sustained release of the antiretroviral efavirenz. Colloids Surf B Biointerfaces 102:441–9.

Shao J, Zheng D, Jiang Z, et al. (2011). Curcumin delivery by methoxy polyethylene glycol-poly(caprolactone) nanoparticles inhibits the growth of C6 glioma cells. Acta Biochim Biophys Sin (Shanghai) 43:267–74.

Sharma R, Walker RB, Pathak K. (2011). Evaluation of the kinetics and mechanism of drug release from econazole nitrate nanosponge loaded carbapol hydrogel. Indian J Pharm Educ Res 45:25–31.

Song Z, Feng R, Sun M, et al. (2011). Curcumin-loaded PLGA-PEG-PLGA triblock copolymeric micelles: preparation, pharmacokinetics and distribution in vivo. J Colloid Interface Sci 354:116–23.

Sun M, Zhao L, Guo C, et al. (2012). Evaluation of an oral carrier system in rats: bioavailability and gastrointestinal absorption properties of curcumin encapsulated PBCA nanoparticles. J Nanoparticle Res 14: 1–13.

Wang Y, Wang C, Gong C, et al. (2012a). Polysorbate 80 coated poly (varepsilon-caprolactone)-poly (ethylene glycol)-poly (varepsilon-caprolactone) micelles for paclitaxel delivery. Int J Pharm 434:1–8.

Wang Y, Wang C, Gong C, et al. (2012b). Polysorbate 80 coated poly (varepsilon-caprolactone)-poly (ethylene glycol)-poly (varepsilon-caprolactone) micelles for paclitaxel delivery. Int J Pharm 434:1–8.

Wurm F, Frey H. (2011). Linear–dendritic block copolymers: the state of the art and exciting perspectives. Prog Polym Sci 36:1–52.

Xie X, Tao Q, Zou Y, et al. (2011). PLGA nanoparticles improve the oral bioavailability of curcumin in rats: characterizations and mechanisms. J Agric Food Chem 59:9280–9.

Xu B, Yuan J, Ding T, Gao Q. (2010). Amphiphilic biodegradable poly(ε-caprolactone)-poly(ethylene glycol)-poly(ε-caprolactone) triblock copolymers: synthesis, characterization and their use as drug carriers for folic acid. Polym Bull 64:537–51.

Yallapu MM, Jaggi M, Chauhan SC. (2010). beta-Cyclodextrin-curcumin self-assembly enhances curcumin delivery in prostate cancer cells. Colloids Surf B Biointerfaces 79:113–25.

Yan Q, Yuan J, Zhang F, et al. (2009). Cellulose-based dual graft molecular brushes as potential drug nanocarriers: stimulus-responsive micelles, self-assembled phase transition behavior, and tunable crystalline morphologies. Biomacromolecules 10:2033–42.

Yen FL, Wu TH, Tzeng CW, et al. (2010). Curcumin nanoparticles improve the physicochemical properties of curcumin and effectively enhance its antioxidant and antihepatoma activities. J Agric Food Chem 58:7376–82.

Yin HT, Zhang DG, Wu XL, et al. (2013). In vivo evaluation of curcumin-loaded nanoparticles in a A549 xenograft mice model. Asian Pac J Cancer Prev 14:409–12.

Zhang Y, Huo M, Zhou J, et al. (2010a). DDSolver: an add-in program for modeling and comparison of drug dissolution profiles. Aaps J 12: 263–71.

Zhang Y, Tang L, Sun L, et al. (2010b). A novel paclitaxel-loaded poly(epsilon-caprolactone)/Poloxamer 188 blend nanoparticle overcoming multidrug resistance for cancer treatment. Acta Biomater 6: 2045–52.

Zhou S, Deng X, Yang H. (2003). Biodegradable poly(epsilon-caprolactone)-poly(ethylene glycol) block copolymers: characterization and their use as drug carriers for a controlled delivery system. Biomaterials 24:3563–70.